Resolution of the fluorescence decay of the two tryptophan residues of *lac* repressor using single tryptophan mutants

Catherine A. Royer,* Joseph A. Gardner,‡ Joseph M. Beechem,§ Jean-Claude Brochon,‖ and Kathleen S. Matthews‡

*University of Illinois Urbana-Champaign, Laboratory for Fluorescence Dynamics, Department of Physics, Urbana, Illinois 61801; ‡Department of Biochemistry and Cell Biology, Rice University, Houston, Texas 77251; §Department of Molecular Physiology and Biophysics, Vanderbilt University, Nashville, Tennessee 37232 USA; and ‖Laboratoire d'Utilisation du Rayonnement Electromagnétique, CNRS-MENJS-CEA, Centre Universitaire Paris-Sud 91405 Orsay, France

ABSTRACT We have studied the time-resolved intrinsic tryptophan fluorescence of the *lac* repressor (a symmetric tetramer containing two tryptophan residues per monomer) and two single-tryptophan mutant repressors obtained by site-directed mutagenesis, *lac* W201Y and *lac* W220Y. These mutant repressor proteins have tyrosine substituted for tryptophan at positions 201 and 220, respectively, leaving a single tryptophan residue per monomeric subunit at position 220 for the W201Y mutant and at position 201 in the W220Y mutant. It was found that the two decay rates recovered from the analysis of the wild type data do not correspond to the rates recovered from the analysis of the decays of the mutant proteins. Each of these residues in the mutant repressors displays at least two decay rates. Global analysis of the multiwavelength data from all three proteins, however, yielded results consistent with the fluorescence decay of the wild type *lac* repressor corresponding simply to the weighted linear combination of the decays from the mutant proteins. The effect of ligation by the antagonistic ligands, inducer and operator DNA, was similar for all three proteins. The binding of the inducer sugar resulted in a quenching of the long-lived species, while binding by the operator decreased the lifetime of the short components. Investigation of the time-resolved anisotropy of the intrinsic tryptophan fluorescence in these three proteins revealed that the depolarization of fluorescence resulted from a fast motion and the global tumbling of the macromolecule. Results from the simultaneous global analysis of the frequency domain data sets from the three proteins revealed anisotropic rotations for the macromolecule, consistent with the known elongated shape of the repressor tetramer. In addition, it appears that the exicted-state dipole of tryptophan 220 is aligned with the long axis of the repressor.

INTRODUCTION

The intrinsic tryptophan fluorescence of proteins has been utilized in the study of a wide variety of biophysical phenomena (e.g., ligand binding, protein re-(de)naturation, protein–protein associations, etc.), primarily due to the two important advantages which fluorescence offers. First, because of the high sensitivity of fluorescence, experiments can be performed at protein concentrations between 10^{-9} and 10^{-5} M, a range in which many biologically important equilibria can be observed. Second, examination of the time-resolved fluorescence intensity and anisotropy decay kinetics of the intrinsic tryptophan residues in proteins (10^{-12} to 10^{-8} s) allows for the observation of dynamic events, such as the diffusion of small ligands, local tryptophan rotations, segmental polypeptide movements, and for relatively small proteins, the brownian rotation of the entire molecule. However, despite the growing interest and large numbers of studies which have been performed, the origins of the complex fluorescence decay patterns observed in proteins are not well understood. For a recent review of tryptophan fluorescence in proteins see Beechem and Brand (1).

Address correspondence to Dr. Royer, School of Pharmacy, University of Wisconsin-Madison, 425 N. Charter St., Madison, WI 53706.

In the case of *two*-tryptophan-containing proteins, several time-resolved fluorescence studies have been performed (2–10), and the fluorescence decay is often resolved into two kinetic components. The observed biexponential decay has been interpreted as arising from the intrinsic monoexponential decay of the two individual tryptophan residues. However, examination of many *single*-tryptophan-containing proteins, reveals that the fluorescence decay of individual residues is not monoexponential (8, 10–18). These results have been interpreted as being due to the intrinsic heterogeneous decay of tryptophan, interaction of the tryptophan residue with charged amino-acid groups of the nearby protein matrix, and conformational heterogeneity of the proteins in solution. Thus, it appears that when a single tryptophan is present in a protein sequence, complex decay of the fluorescence of this single residue is often observed. When two-tryptophan-containing proteins are examined, the fluorescence decay appears "less complex" due to the collapsing of many of the exponential components into single kinetic terms. This result is not unexpected, given the inherent difficulty in resolving complex multiexponential decay. In fact, it seems that, depending upon the degree to which the multiple decays present in the protein emission are dissimilar, they may or may not be resolved by current

0006-3495/90/08/363/16 $2.00

analysis methodology. It therefore appears that the two decay components which are often observed for two-tryptophan proteins may actually be composed of a complex average of the multiexponential decay kinetics of each emitting tryptophan. The examination of the fluorescence decay characteristics of *E. coli lac* repressor (a symmetric tetrameric two-tryptophan-containing protein with predominately biexponential decay kinetics) and each of its single-tryptophan-containing mutants (obtained by site-directed mutagenesis) provides a powerful tool with which to test his hypothesis. We point out that at the concentrations of repressor proteins used in this experiment, ~2 μM in tetramer, the wild type *lac* repressor is known to be completely in its tetrameric form. The dissociation constant for the dissociation to dimer has been measured by high pressure techniques (19) and was found to be between 10 and 15 nM. We are thus at a concentration which is 100–200-fold the K_d. The subunit affinity of the mutant proteins has not been determined, but each behaves identically to the wild type in molecular sieve chromatographic experiments at concentrations of near 10 μM in tetramer. Thus, dissociated *lac* repressor species have no significant contribution to the fluorescence signal in the present experiments. It has also been shown (20) that the tryptophan intensity and emission energy are not sensitive to the oligomeric state of the protein.

Previous studies by Brochon and co-workers (5) of the intrinsic fluorescence decay of wild type *lac* repressor showed biexponential decay behavior with lifetimes of 3.8 and 9.8 ns. Examination of the decay kinetics of the fluorescence at multiple emission wavelengths revealed that the steady-state fluorescence spectrum could be decomposed into a blue-shifted component (associated with the 3.8-ns lifetime) and a red-shifted component (associated with the 9.8-ns lifetime). These two components were postulated to correspond to the two different tryptophan residues in the protein. Upon binding of the inducer sugar, isoprophyl-β-D-thiogalactoside (IPTG), the lifetime of the long component decreased to 7.6 ns and its spectrum shifted 11 nm to the blue. Studies of the steady-state fluorescence emission spectra of mutants lacking tryptophan 220 or 201 (21) demonstrated that the spectrum of the mutant lacking 220 had its emission maximum 13 nm to the blue of that lacking tryptophan 201. On this basis, the red (long) component was assigned to tryptophan 220 and the blue (short) component was assigned to tryptophan 201 (5). In the following study we have examined the time-resolved fluorescence of the intrinsic tryptophan emission of the wild type *lac* repressor and of two mutant proteins, W201Y and W220Y, which have tyrosine substituted for the tryptophan at positions 201 and 220, respectively (Gardner, J. A., and K. S. Matthews, manuscript in preparation). We were interested in determining whether the mutant proteins would display single exponential decays, corresponding to the two lifetimes recovered by Brochon and co-workers (5) for the wild-type *lac* repressor. In addition, the effect of ligation by the inducer sugar and the specific operator sequence upon the fluorescence decay have been investigated. Because the antagonism between these two ligands is the basis for the control of the expression of the genes in the *lac* operon, the changes upon the fluorescence decay associated with their binding were of particular interest in relating the activity of the macromolecule and the characteristics of its tryptophan residues. To compare the dynamic properties of the wild type repressor with those of the mutants with the goal of resolving the rotational properties of the two-tryptophan residues, we also examined the time-resolved anisotropy of the three proteins.

MATERIALS AND METHODS

Proteins

Mutant repressor proteins with tyrosine substituted for tryptophan have been produced previously by suppression of amber mutations (21), but these strains yielded low levels of protein and were very unstable. Therefore, site-specific mutagenesis techniques (22) were utilized to create two mutant repressors, each containing a single tryptophan (Gardner, J. A., and K. S. Matthews, manuscript in preparation). Oligomers of 23 bases were synthesized complementary to the repressor anti-sense strand sequence surrounding each tryptophan residue codon, except that the trp codons (CCA) were changed to those coding for tryosine (ATA). The oligonucleotides were annealed to single-stranded uracil-containing pAC1 (Chakerian, A. E., and K. S. Matthews, manuscript in preparation), a plasmid created by inserting a wild-type *lac* gene into the unique *Eco RI* site in pEMBL 9+ which confers ampicillin resistance (23). After elongation in the presence of the four dNTPs and ligation, the mixture was used to transform competent *E. coli* 71-18 cells. The ssDNA was isolated and sequenced using the Sanger dideoxy method (24). The ssDNA that gave the sequence expected for the mutant repressors was then used to transform competent *E. coli* PD8 cells. Ampicillin-resistant PD8 cells were assayed for the ability to bind IPTG, and those cells exhibiting the highest levels of binding were grown in 15-liter batches. Plasmid isolated from these cells was sequenced to confirm the presence of a single mutation at the desired site. Harvested cells were frozen in the presence of lysozyme (10–15 mg/100 g cells). Mutant repressors were isolated following the same procedures as for wild-type repressor (25). Purity of isolated protein was >90% as determined by SDS-PAGE and silver staining. The operator binding affinities in the two mutants are lower than that measured for the wild-type protein, by factors of ~5 and 10 for the W220Y and W201Y mutants, respectively. Inducer binding was identical to wild type for the W201Y mutant. However, inducer affinity was reduced almost 30-fold for the W220Y mutant, indicating that this tryptophan may reside in or near the inducer binding site. Fluorescence measurements were carried out using <0.1 OD units of protein measured at 295 nm to avoid trivial reabsorption effects. Buffer was 100 mM KCl, 100 mM Tris, pH 7.1, and 10^{-4} M DTT.

Instrumentation

Time-domain fluorescence decay measurements were carried out using the time-correlated single photon counting technique (26–28). The excitation light pulse source was the synchrotron radiation emitted by the new positron storage ring Super-ACO used in the two-bunch mode. The corresponding repetition rate was 8.25 MHz. A previous experimental set-up (29–31) was modified to fit with the new excitation source (Brochon, J. C., F. Mérola, J. Gallay, and M. Vincent, manuscript in preparation). Using JY 25 monochromators (Jobin-Yvon, Longjumeau, France) vertically polarized excitation was set at 296 nm (d − λ = 6 nm), and the emission monochromator was set at either 340 or 400 nm (d − λ = 6 nm). The two components I_{vv} and I_{vh} were recorded, and the total fluorescence decay corresponds to the weighted sum of the two components:

$$I(t) = I_{vv}(t) + [2\beta I_{vh}(t)], \quad (1)$$

where β is a correction factor for the transmission of polarized light by the monochromator at a given wavelength. The channel width was 63.9 ps/channel, and data were collected in 1,023 channels. With a stored amount of particles corresponding to a current of 30 mA, the instrument response function determined from a scattering solution of Ludox was typically 0.75 ns (FWHM) using a model XP2020Q photomultiplier (Philips Electronics, Eindhoven, Netherlands). Each measurement typically required 40 min of data collection and contained 5–15 × 10^6 total counts.

The frequency responce of the *lac* wild-type protein and the two mutant repressor proteins was measured using the cross-correlation phase and modulation fluorometer described by Alcala et al. (32). The response at multiple frequencies was obtained by cross-correlation with the harmonic content of 2 MHz pulses from a mode-locked frequency doubled Nd-YAG laser (model 76-S) coupled with a cavity-dumped dye laser (models 7220 and 702), and external frequency doubler (model 7049) all from Coherent Corp. (Palo Alto, CA). The excitation wavelength was set at 295 or 305 nm by adjusting the birefringent crystal of the dye laser. Phase and modulation data for the protein solutions were obtained at emission wavelengths of 320, 340, 360, 380, and 400 nm using a monochromator (ISA Instruments, Edison, NJ) with slits of 2 mm (bandpass 8 nm). When a cuton emission filter was used it was a WG-320 from Schott Optical Glass, Inc. (Duryea, PA). The reference compound, para-terphenyl in cyclohexane, was utilized to correct for the color shift and instrumental phase delay of the detection equipment (lifetime = 1 ns). The error on the phase angles and demodulation factors was <0.6 degrees and 0.004, respectively.

Analysis

The frequency domain multiwavelength data were analyzed using the global analysis software package, Globals Unlimited (University of Illinois, Urbana, IL), which is based on theory and algorithms described elsewhere (33–36). These algorithms allow for the simultaneous analysis of multiple data sets in terms of internally consistent sets of kinetic models. In the time domain, the analysis of $I(t)$ as a sum of exponentials was performed by the maximum entropy method (MEM) described by Livesey and Brochon (37). The theory and general algorithm of MEM have been previously published (38, 39). The initial lifetime components were equally spaced in logarithmic scale, 100 lifetimes ranging from 0.05 to 25.0 ns.

RESULTS

Lifetime results

The frequency responses of wild type *lac* repressor fluorescence (exciting at 295 nm) obtained at multiple emission wavelengths is shown in Fig. 1 *a*. It can be seen that as the wavelength of observation increases, the frequency response shifts to lower frequencies, indicating increased fluorescence due to a long-lived component on the red edge of the spectrum. The data from all wavelengths were simultaneously analyzed as a double exponential decay using a linkage scheme in which the lifetime across the emission spectrum were considered invariant, but the fractional contributions of each component to the total intensity (f_i) were allowed to vary. The Global Unlimited software allows for direct fitting for either the amplitudes, α, or the weighted $\alpha - \tau$ products, f_i. The latter fractional intensities are used to directly calculate the decay associated spectra (DAS). The lifetime values recovered from this analysis, 9.85 and 3.27 ns, were very close to those reported earlier by Brochon et al. (5) (9.8 and 3.8 ns). The global χ-square for this fit was 1.72. Phase and modulation residuals for the five data sets shown in Fig. 2 indicate random deviations between the calculated and measured values. The fractional contribution of the long-lived component increases from 58% at 320 nm to 97% at 400 nm. Fig. 1 *b* shows the decay-associated spectra (DAS) for the two lifetime components. These DAS are obtained by multiplying the fractional intensity, f_i, for a given component recovered from the analysis for a given emission wavelength by the total steady-state emission intensity at that wavelength. The short component spectrum shows a maximum at 320 nm whereas the long component maximum is found at 340 nm. These results are quite similar to those reported previously for the wild-type protein by Brochon et al. (5). Rigorous error analysis (35, 36) performed on the recovered lifetime values and shown in Fig. 3, *a* and *b* revealed that the value of the short component can be considered to lie between 3.05 and 3.50 ns, whereas that of long-lived component lies between 9.56 and 10.10 ns (at the 67% confidence level).

The same multiemission wavelength experiments were conducted on the mutant proteins, W220Y (with tyrosine substituted for tryptophan 220) and W201Y (with tyrosine substituted for tryptophan 201). The phase and modulation data as a function of wavelength for these two proteins are shown in Fig. 1, *c* and *e*. A small wavelength dependence is evident for both mutant proteins indicating that neither decays as a single exponential, independent of wavelength. In fact, single exponential fits of the multiwavelength data yielded chi-square values in excess of 35.

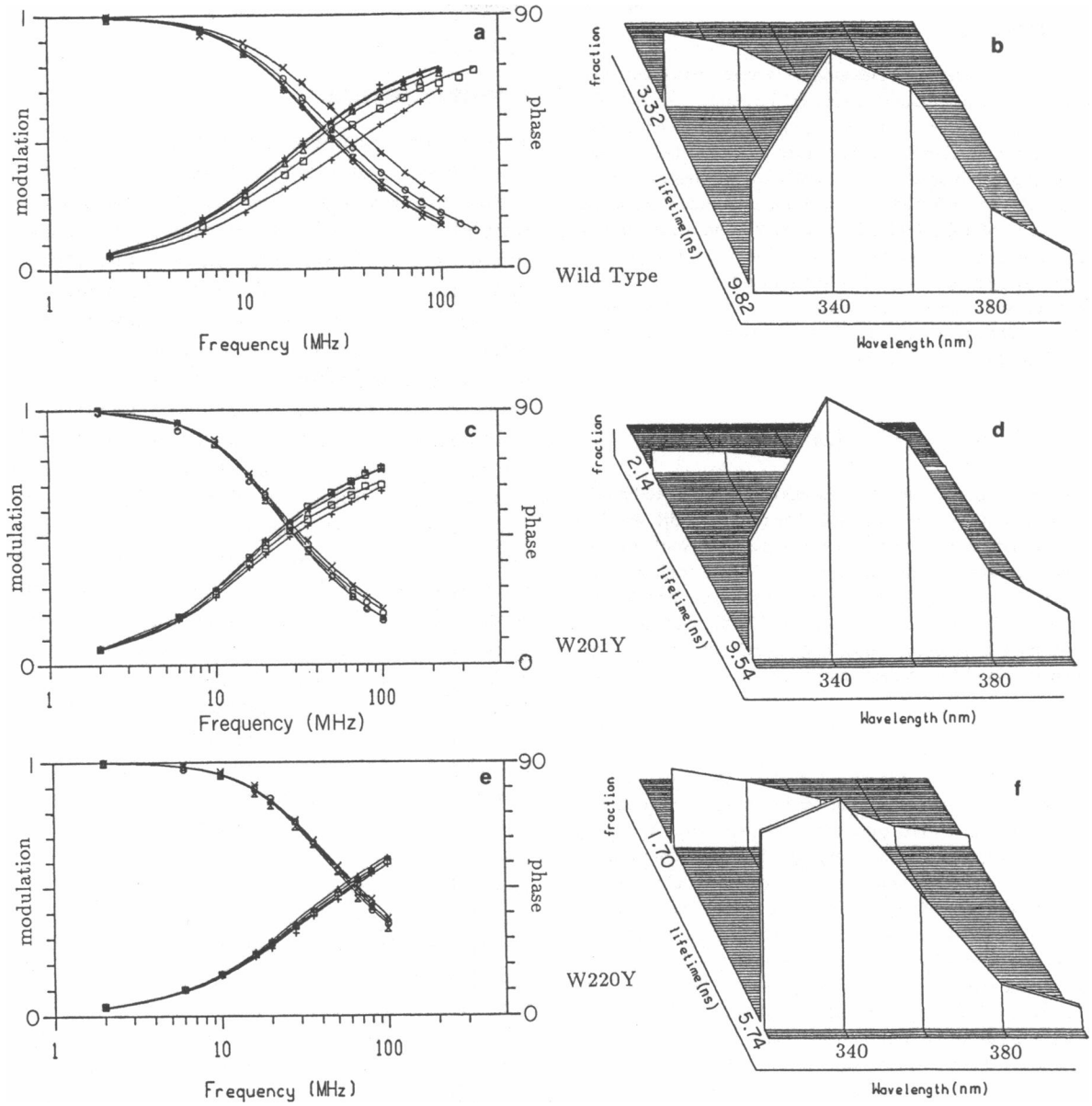

FIGURE 1 Frequency response with double exponential global analyses at 320, 340, 360, 380, and 400 nm in emission and recovered decay associated spectra for (*a* and *b*) wild-type *lac* repressor, (*c* and *d*) *lac* W201Y, and (*e* and *f*) *lac* W220Y. The curves show demodulation and phase shift at lower frequencies as the emission wavelength is moved toward the red.

When the multiple wavelength data from the mutants were analyzed globally as double exponential decays, the χ^2 values decreased to 2.54 and 1.53, respectively, for the W220Y and W201Y mutants. Analysis in terms of triple exponentials resulted in no further decrease in the χ^2 values. The lifetime values recovered for the W220Y mutant were 5.88 and 1.81 ns, with the long component displaying a more red-shifted spectrum. The analysis of the data from the W201Y mutant yielded lifetime values of 9.43 and 2.01 ns. Decay-associated spectra for the mutant *lac* repressor proteins are shown in Fig. 1, *d* and *f*. The 9.43-ns component in the *lac* W201Y had a very red-shifted spectrum with an emission maximum at 340 nm, similar to the decay-associated spectrum of the 9.85 ns component in the wild type. In addition, a small short component is evident with a very blue-shifted spectrum. The 5.88-ns component of the W220Y mutant shows a maximum at 340 nm, although the spectrum is slightly blue-shifted compared to that of the 9.85-ns component in either the wild type or the W201Y mutant. As in the case

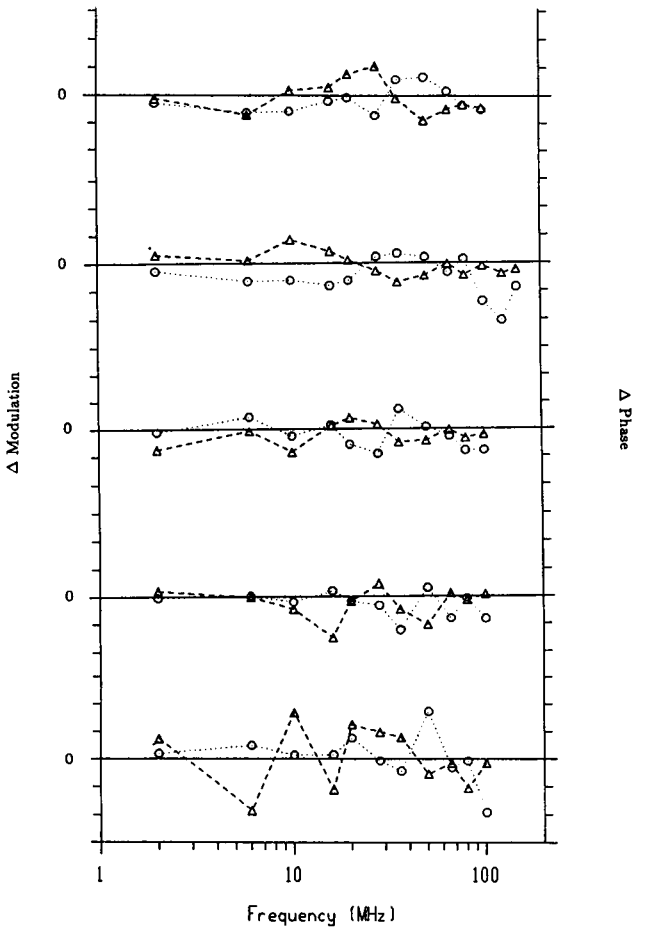

FIGURE 2 Phase and modulation residuals for the double exponential global analysis of the wild-type *lac* repressor at (*a*) 320, (*b*) 340, (*c*) 360, (*d*) 380, and (*e*) 400 nm. Full-scale deviations are 3 degrees of phase and 0.05 in modulation. Circles correspond to the phase residuals, triangles to the modulation.

of the W201Y mutant, the short component maximum in the W220Y mutant is found at 320 nm. Residuals from these fits are shown in Figs. 4 and 5. Rigorous error analysis was performed on the recovered lifetimes for the two mutants and the confidence interval plots are shown in Fig. 3, *c–f*. The value of the long-lived component in the *lac* W201Y mutant can be seen to lie between 9.25 and 9.62 ns at the 67% confidence level and corresponds well to the 9.85-ns component found in the wild-type repressor. The shorter, blue component of this mutant has a lifetime between 1.73 and 2.29 ns. As for the W220Y mutant, neither lifetime corresponds to the 3.32-ns component recovered from the wild-type data. The longer lifetime component in the mutant lacking tryptophan 220 displays a value which lies between 5.51 and 6.32 ns, whereas the shorter component exhibits a value between 1.59 and 2.03 ns. The results of the double exponential fits of the frequency response data are summarized in Table 1.

The intensity decay curves of these same proteins were obtained using the single photon counting technique at 340 and 400 nm emission and analyzed using the maximum entropy method (MEM) (37). Typical decay curves at 340 nm for the wild type and the W220Y and W201Y mutants are shown in Fig. 6, *a–c*. The lifetime distributions recovered from the maximum entropy distributions for the wild type at 340- and 400-nm emission are shown in Fig. 7, *a* and *b*. The maximum entropy distributions at 400 nm for the two mutant proteins are shown in Fig. 7, *c–f*. The recovered molecular concentration and mean lifetime values from the distributed peaks are reported in Table 2. These fits were carried out in terms of the amplitude, α, as opposed to the global fits which were done in terms of the fractional intensity of each component. Again, there was less wavelength dependence for the two mutant proteins than for the wild-type protein. The wild-type *lac* repressor exhibits a 9.75 ns component with a molecular fraction (α) which increases from 55 to 94% between 340 and 400 nm and a 3.31-ns component with a molecular fraction (α) which decreases from 39 to 0% over the same wavelength range. These results are in very good agreement with those from the frequency domain data. However, a small amount ($\alpha = 6\%$) of a short component. ~0.9 ns, was recovered from both data sets. Analysis by MEM of the data from the *lac* W220Y mutant also yielded three components, two of which (5.21 and 1.82 ns) agreed with the values recovered from the frequency domain data. Approximately 50 and 15% (in terms of α) of a shorter component (140 ps) was also recovered. A long component (9.05 and 9.55 ns at 340 and 400 nm emission, respectively) is evident in the *lac* W201Y results, clearly equivalent to the long component recovered from the frequency domain data for the same sample. MEM also yielded two shorter blue-shifted components (0.11 or 1.5 ns and 2.2 and 3.8 ns for the 340- and 400-nm experiment, respectively). All of these values were in or very near the solution space found from the global multiwavelength analysis. The resolution of these experiments both at short times and high frequencies is not adequate for determining whether the very short components recovered from the single photon counting data are significant. Even the recovered amplitude of 50% for the 140-ps component in the W220Y mutant is only responsible for 3% of the total intensity, which is the measured quantity.

From the above results it is apparent that the component which displays a fluorescent lifetime of ~9 ns is well resolved in the wild-type repressor and in the *lac* W201Y mutant and clearly corresponds to the major fraction (but not all) of the emission from tryptophan 220. In addition, this tryptophan does not decay as a single exponential, as

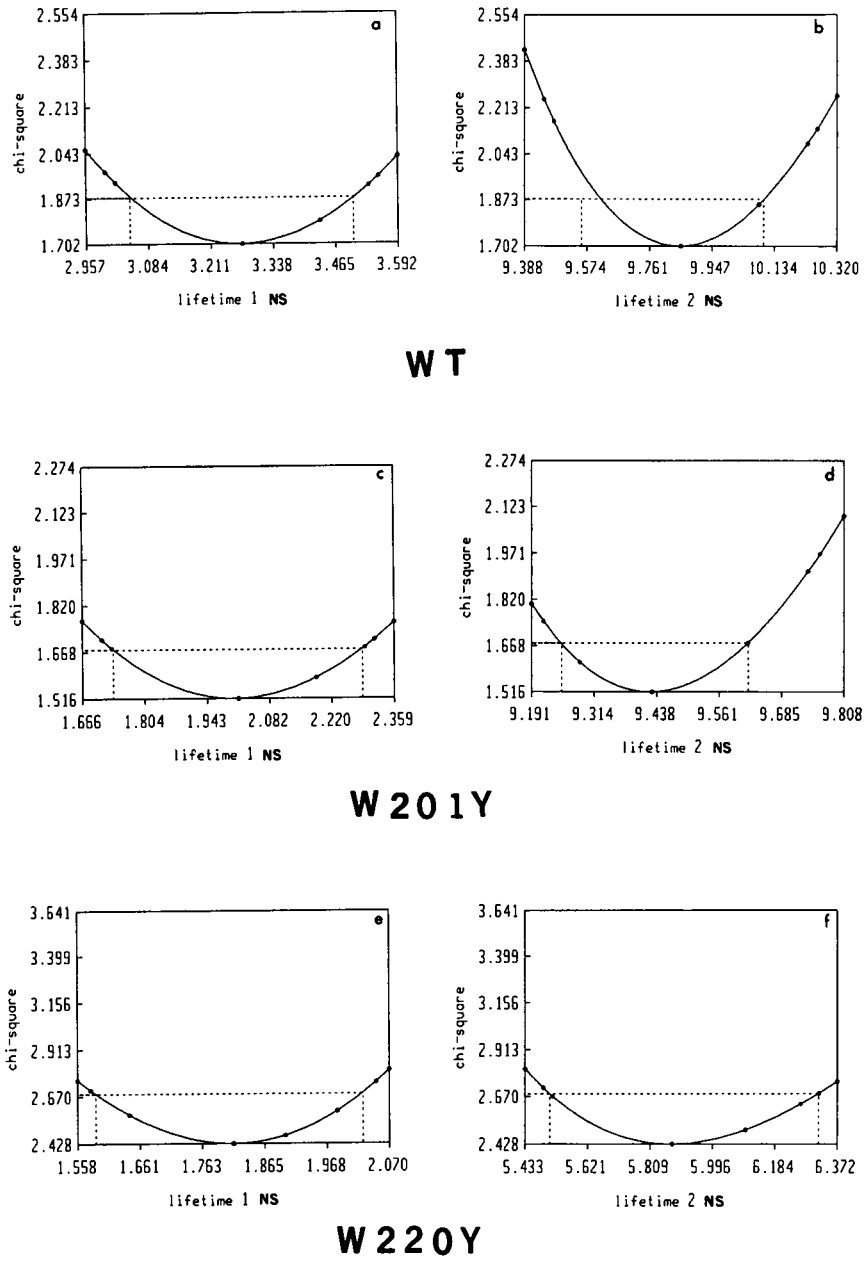

FIGURE 3 Confidence interval plots for the two lifetimes recovered from the double exponential decay global analysis of the multiple emission wavelength data from (*a* and *b*) wild-type *lac* repressor, (*c* and *d*) *lac* W201Y, and (*e* and *f*) *lac* W220Y. Lines are drawn horizontally through the 67% confidence level which represents one standard deviation of the data. The actual recovered confidence limits are reported in the text.

has been shown for a number of single-tryptophan proteins. The global nonlinear least squares analysis of the frequency domain data from the W201Y mutant yielded one additional component near 2 ns, whereas the MEM analysis of the time domain data gave two additional components, one at 3 ns and the other at 1 ns. The decay of tryptophan 201 (*lac* W220Y) was not monoexponential either. Neither recovered lifetime (~5 and 2 ns) corresponds to the 3-ns component recovered in the double exponential analysis of the wild-type repressor. It appears that the analysis of the wild-type repressor results in the collapse of the components from each tryptophan (except the well-resolved 9-ns emission) into a single lifetime of ~3 ns. Apparently the multiple decay rates from the tryptophan residues in the two mutants were present in the wild-type data but were not resolvable. Analyzing the wild-type repressor as a triple exponential decay (again linking lifetimes across the emission spectrum) yielded a 9.8-ns component which was red shifted in the same manner as found for the double exponential decay. A

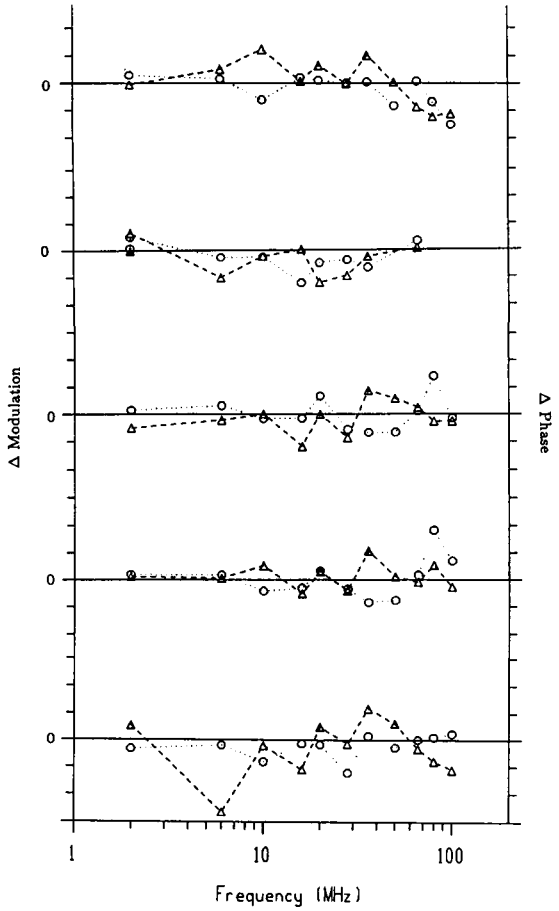

FIGURE 4 Phase and modulation residuals for the double exponential global analysis of the multiple emission wavelength data from *lac* W201Y at (*a*) 320, (*b*) 340, (*c*) 360, (*d*) 380, and (*e*) 400 nm. Full scale deviations are 3 degrees of phase and 0.05 in modulation. Circles correspond to the phase residuals, triangles to the modulation.

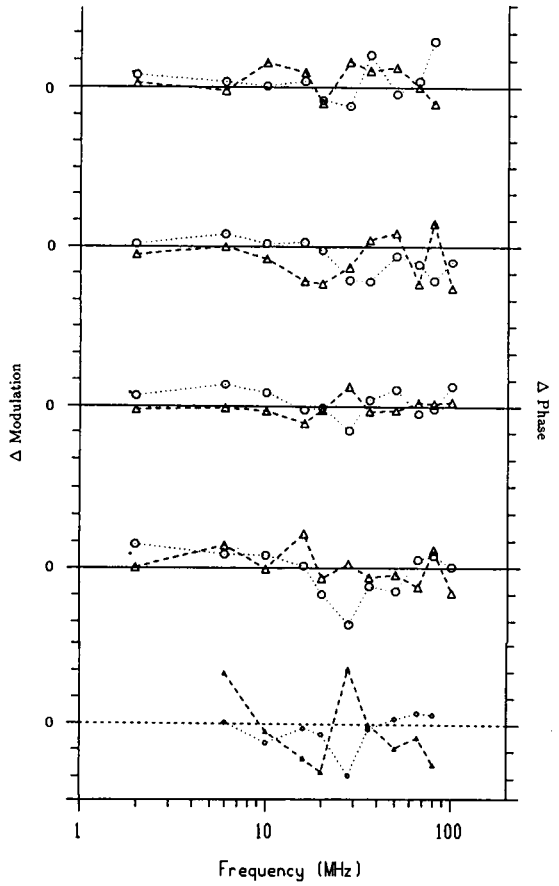

FIGURE 5 Phase and modulation residuals for the double exponential global analysis of the multiple emission wavelength data from *lac* W220Y at (*a*) 320, (*b*) 340, (*c*) 360, (*d*) 380, and (*e*) 400 nm. Full scale deviations are 3 degrees of phase and 0.05 in modulation. Circles correspond to the phase residuals, triangles to the modulation.

3.7-ns component and 670 ps component with emission maxima at 320 nm were also recovered. The short component recovered here is similar to that seen in the MEM analysis. The 5-ns component recovered from the *lac* W220Y mutant was again not evident. It can be seen from the confidence interval plots shown in Fig. 8, *a–c*, that all three components exhibit very shallow minima, and that the lifetimes recovered for the two mutant proteins lie within the solution space (at the 67% confidence level) of the wild-type data. For the number of degrees of freedom in this analysis, the 67% confidence interval considers as possible solutions, all sets of amplitudes and lifetimes with χ^2 values less than or equal to 1.94. For instance, the solution obtained for lifetime values of 2.4, 5.0, 9.8 corresponds to a χ^2 value of 1.85, well within the possible set of solutions.

If the two tryptophans in the native protein are noninteracting (no excitation wavelength dependence of the decay was observed between 295 and 305 nm) and the local structure is unchanged by the mutation, then the observed fluorescence decay of the wild-type protein should simply correspond to the linear weighted superposition of the decay kinetics of the two mutant proteins. The existence of the two mutant proteins (along with the wild type) allows for the possibility of testing this hypothesis by performing a global simultaneous analysis of the complete multiemission wavelength studies of the three different proteins (both mutants and wild type). In this global analysis, double exponential lifetimes for each mutant were linked across the multiple emission wavelengths. In addition, the fluorescence decay of the wild-type protein was linked across the emission wavelengths and constrained to be composed of linear combinations of the sets of lifetimes from the two different mutant proteins. The resultant simultaneous fit and data from all

TABLE 1 Frequency response of the wild-type and mutant *lac* repressor proteins: Results of global analysis

Protein	τ_1	τ_2	χ^2
Wild type	9.85 + 0.25/−0.30	3.27 + 0.23/−0.23	1.72
W220Y	5.88 + 0.43/−0.37	1.81 + 0.22/−0.22	2.24
W201Y	9.43 + 0.19/−0.18	2.01 + 0.28/−0.28	1.53

Excitation was at 295 nm. Data sets taken at five different emission wavelengths (320, 340, 360, 380, and 400) were analyzed simultaneously for each protein for an internally consistent set of fluorescence lifetimes. Fractional contributions of the individual components were allowed to vary between data sets, while the lifetime values were linked across the data sets. The recovered fractional intensities were used to calculate the decay-associated spectra.

three proteins is shown in Fig. 9 *a*. It can be seen that the wild-type data is bounded by that of the two mutants, and that it is closer to the W201Y because the long-lived tryptophan contributes more to the fluorescence signal. The global analysis of these data reveals that the fluorescence decay of the wild-type protein can be decomposed into (at least) four lifetimes of 1.7, 2,2, 5.8, and 9.6 ns (global $\chi^2 = 3.0$). The fractional intensity values for the 1.7- and 2.2-ns lifetime components in the wild-type repressor, however, cannot be uniquely recovered. Only the sum of these two terms was found to be constant. As a result, the decay associated spectra of the wild-type protein can be uniquely decomposed into only three distinct DAS (not four). These decay-associated spectra calculated using the fractional intensities recovered from this fit are shown in Fig. 9 *b*. Both the 2- and 5.8-ns components are blue shifted with respect to the 9.6-ns component. Thus, although not evident from analysis of the data from the three proteins separately, this global-linked analysis of the wavelength dependence of the frequency response of the wild type and the two mutants indicates that the fluorescence of the wild type is consistent with a weighted sum of the fluorescence from the two mutants.

Effect of ligation on the decay parameters

The effect of ligation upon the fluorescence decay parameters of the wild-type repressor and the two mutant repressors was investigated. A WG320 cut-on filter was used in emission to study the decay over the entire spectrum. The effect of saturating IPTG on the frequency response of the wild-type tryptophan emission is shown in Fig. 10 *a*. It can be seen that the data at low frequencies are most strongly affected by inducer binding. Upon addition of IPTG, the 9.69-ns component decreases to 7.42 ns (23%). Again, these results are very similar to those reported by Brochon and co-workers (5). In contrast, addition of saturating 40–base pair oligonucleotide containing the operator sequence results in a change in the high-frequency points (Fig. 10 *b*). Analysis yielded a slight decrease in the value of the long component upon operator binding and a 29% decrease in the value of the short component.

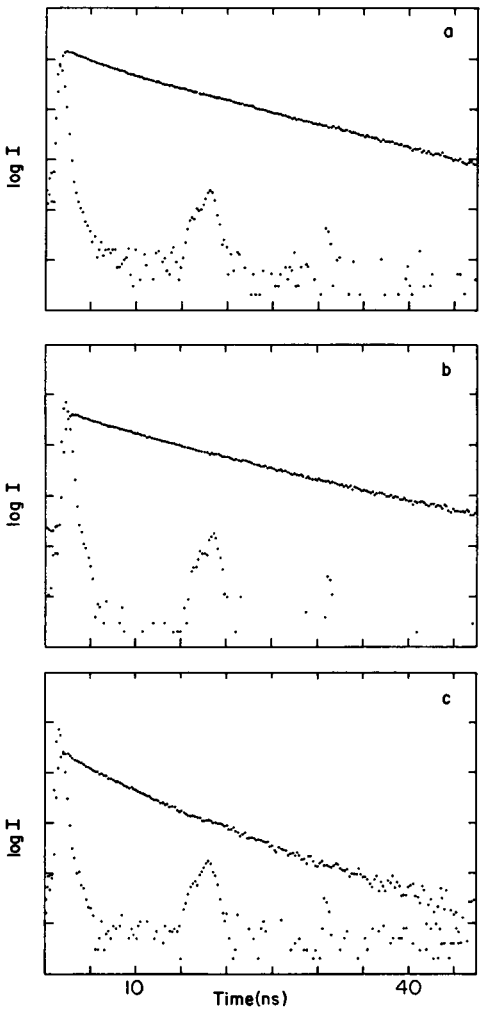

FIGURE 6 Intensity decay curves exciting at 296 and monitoring emission at 340 nm for (*a*) wild-type *lac* repressor, (*b*) *lac* W201Y, and (*c*) *lac* W220Y.

The effect of ligation on the decay of the mutant proteins is shown in Fig. 10 *c–f*. As in the case of the wild type, there is a large change in the low frequency data points for the W201Y mutant upon inducer binding. The long-lifetime component decreases in value by 19%. The high-frequency points are most affected by operator binding (30% decrease in the value of the short lifetime). The effect of ligation is suprisingly quite similar on the fluorescence of the W220Y mutant, with operator further

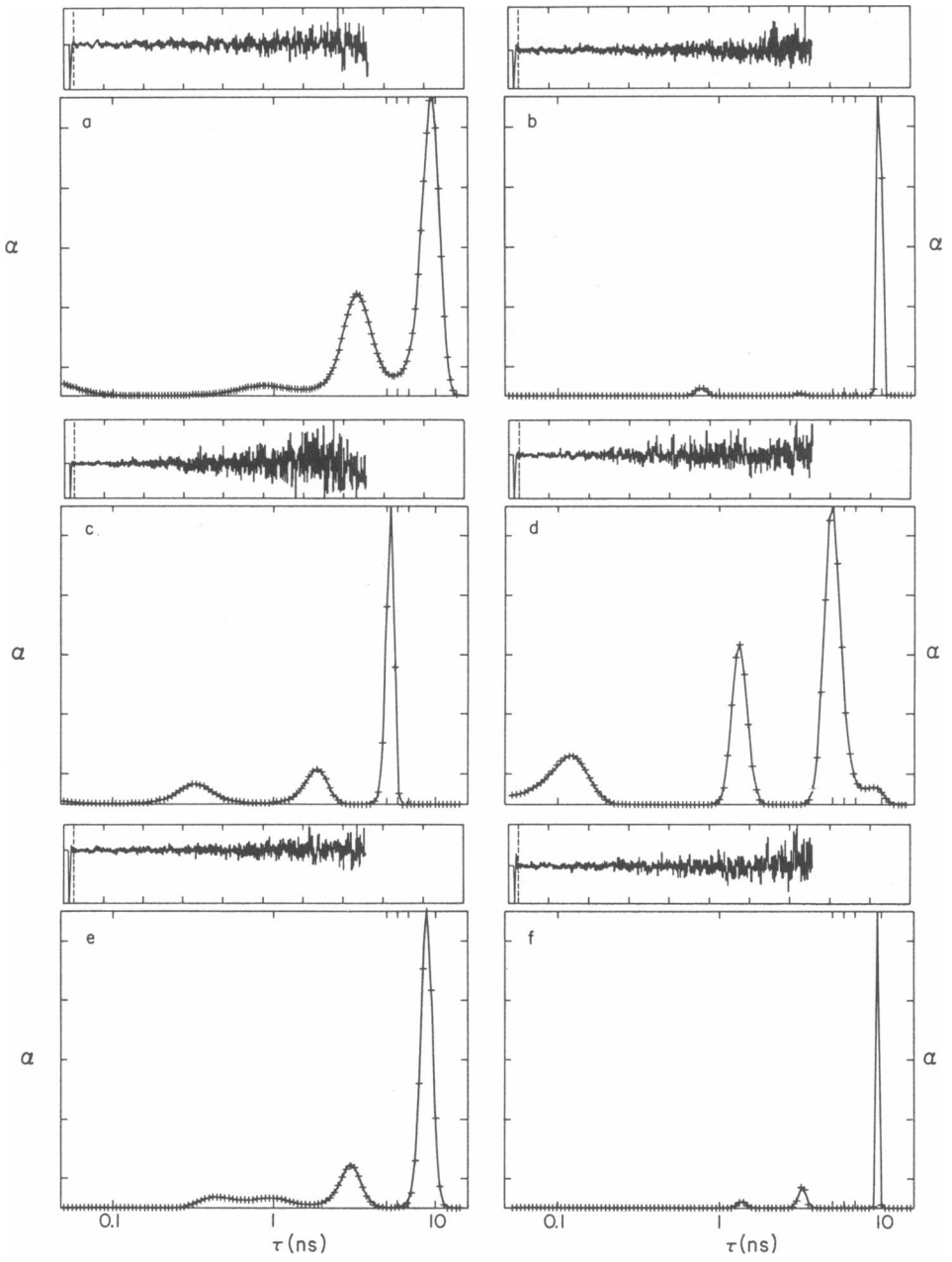

FIGURE 7 Recovered maximum entropy distributions from the intensity decay curves monitored at 340 and 400 nm in emission for (*a* and *b*) wild-type *lac* repressor, (*c* and *d*) W201Y *lac*, and (*e* and *f*) W220Y *lac*. The residuals shown here are the unweighted residuals. However, the weighted residuals, as used in the MEM analysis also showed only random deviations.

quenching the short component. Inducer binding in this mutant results in a decrease in the value of both components. The results of the analyses are summarized in Table 3. Due to the different emission optics and the fact that only one curve was analyzed for each ligand, the recovered lifetime values are not exactly those reported in Table 1. However, they all lie within (or quite near) the solution space of the values in Table 1 (at the 67% confidence level).

Time-resolved anistropy

Differential polarization measurements were carried out on the wild type *lac* repressor and the two single-

TABLE 2. Time response of the wild-type and mutant *lac* repressor proteins: results of the maximum entropy analysis

Protein	λ_{em}	τ_1	τ_2	τ_3	α_1	α_2	α_3	χ^2
Wild type	340	0.88	3.31	9.75	0.06	0.39	0.55	2.01
	400	0.88	—	9.75	0.06	—	0.94	1.22
W220Y	340	0.14	1.82	5.21	0.50	0.13	0.37	1.17
	400	0.14	1.3	5.23	0.15	0.25	0.60	1.01
W201Y	340	0.11	2.20	9.05	0.33	0.15	0.52	1.57
	400	1.50	3.80	9.55	0.07	0.14	0.79	1.10

Excitation was at 295 nm. Emission was monitored at either 340 or 400 nm through a monochromator with 8-nm slits.

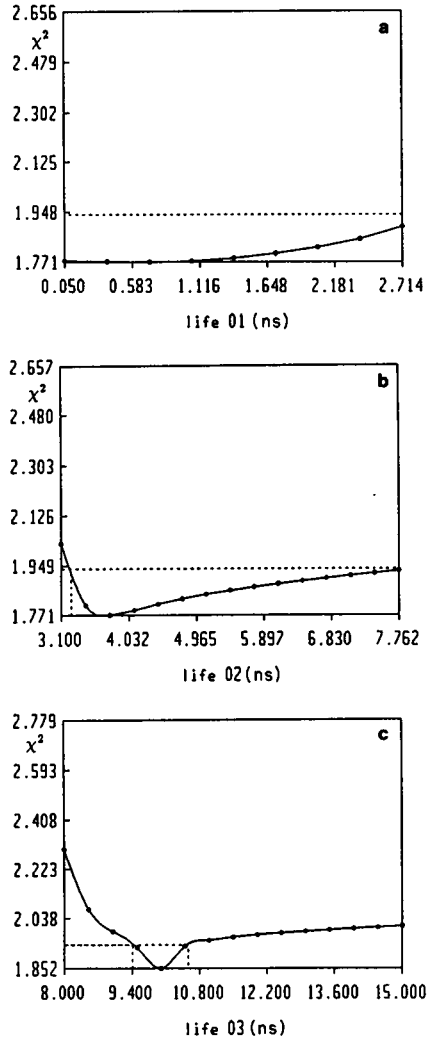

FIGURE 8 Confidence interval plots on the recovered lifetimes from a triple-decay global analysis of the multiple wavelength wild-type frequency domain data. Dotted lines represent the 67% confidence level, which is one standard deviation of the data.

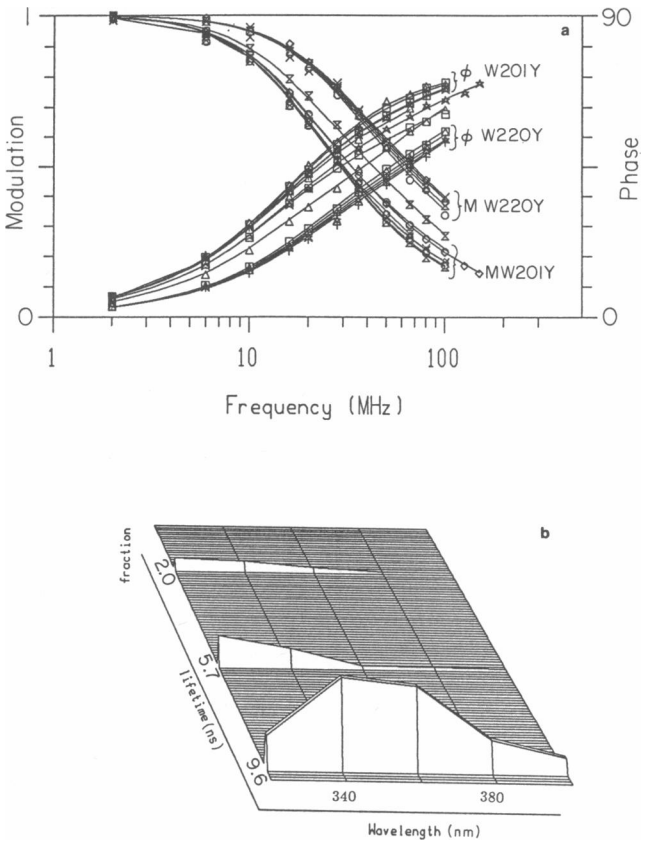

FIGURE 9 (*a*) Frequency repsonse and global fit of the multiwavelength frequency domain data from all three proteins assuming double exponential decays for the two mutants and a quadruple decay with the mutant lifetime values for the wild-type *lac* repressor. The cluster of curves which cross at high frequencies (~70 MHz) correspond to the frequency response of the W220Y mutant repressor. Those which cross at low frequency (~30 MHz) correspond to the data taken on the W201Y mutant repressor. The curves which are distributed in between these two clusters correspond to the wild-type repressor response. (*b*) Decay-associated spectra for the wild-type repressor using the fractional intensities (f_i) recovered from this fit. Fractional intensities from the two short components were summed. See explanation in the text.

tryptophan mutants using a WG320 cuton filter in emission. The data from these experiments are shown in Fig. 11 *a*. Single curve nonlinear analysis yielded a 45-ns correlation time for the wild type (Fig. 11 *a*) with a preexponential factor, β, of 0.275, corresponding to 86% of the total depolarization and a small amount of a very fast rotation (59 ps) with a preexponential factor, β, of 0.045, corresponding to 14% of the total depolarization. Single curve analysis of each mutant protein again yielded a long correlation time, corresponding to the global tumbling of the macromolecule and a very fast rotation, around 90 ps, which was responsible for ~20% of the total depolarization. The recovered values are summarized in Table 4. It should be noted that the long

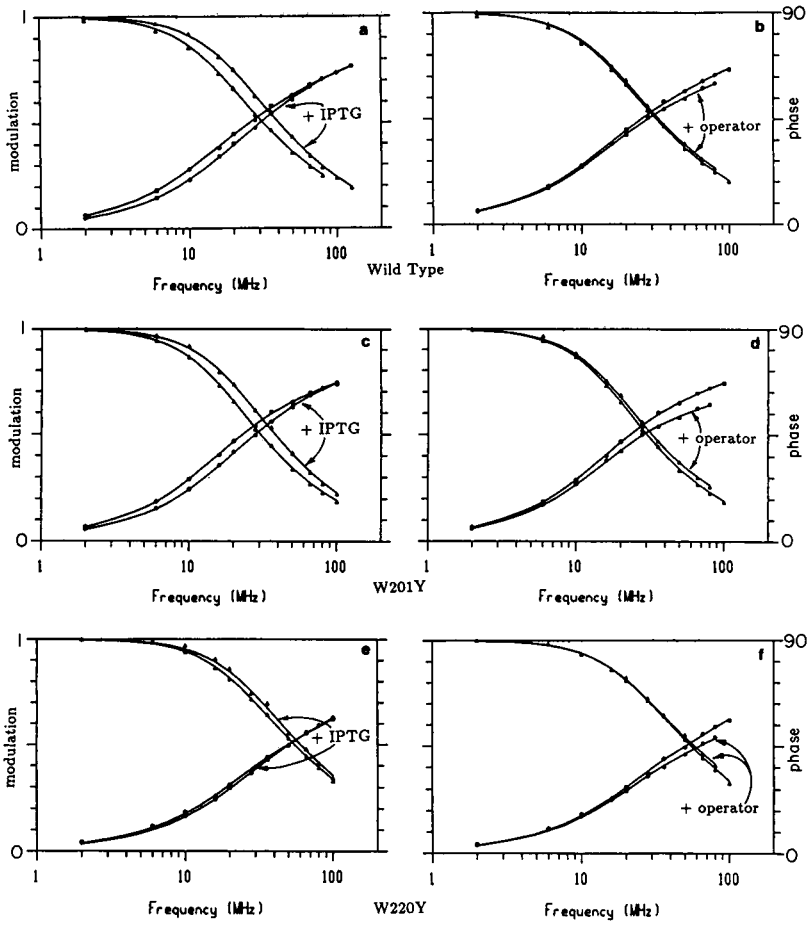

FIGURE 10 The effect of ligand binding on the frequency response of the repressor proteins using WG 320 cuton emission filters to monitor the entire spectrum, (*a* and *b*) IPTG and operator, respectively, bound to wild-type *lac;* (*c* and *d*) IPTG and operator, respectively, bound to *lac* W201Y; and (*e* and *f*) IPTG and operator, respectively, bound to *lac* W220Y. The phase shift and demodulation curves in each figure which are shifted to higher frequency correspond to ligated protein, the other to the unligated control.

rotational correlation time recovered from the wild-type data is much lower than that recovered from the W201Y mutant. The value obtained from the W220Y mutant is intermediate. If the *lac* repressor had a perfect spherical shape, the slow rotational correlation time associated with the overall protein tumbling motion should be identical for the wild-type enzyme and each mutant. However, for asymmetric molecules, the recovered slow rotational correlation time will be different for each protein species examined, due to the fact that each tyryptophan may have a different set of angles between their absorption/emission oscillator and the principal diffusion axes of the protein. For instance, tryptophan residues aligned along an equatorial position (along the short axis) are depolarized by both "tumbling" (end over end) and "spinning" (about the long axis) motions, whereas residues aligned along the long axis are sensitive to only tumbling motion. Hence, trypotphan residues aligned along the long axis

TABLE 3 Effect of ligation on the time-resolved fluorescence of wild-type and mutant *lac* repressor proteins: decay parameters recovered from frequency response data

Protein	Ligand	τ_1	f_1	τ_2	f_2	χ^2
Wild type	—	9.69	0.860	2.76	0.140	4.75
	IPTG	7.42	0.882	2.81	0.118	2.16
	Operator	9.28	0.862	2.02	0.138	2.57
W201Y	—	9.51	0.930	2.06	0.070	3.07
	IPTG	7.65	0.926	2.35	0.074	3.70
	Operator	9.09	0.885	1.44	0.115	4.75
W220Y	—	6.41	0.741	1.84	0.259	6.46
	IPTG	5.17	0.855	1.30	0.145	7.55
	Operator	6.31	0.731	1.41	0.269	4.25

Excitation was at 295 nm. Emission was monitored using a WG320 cuton filter. Data were analyzed as single curves for a two-component decay in terms of the lifetimes and their respective fractional intensities (f_i). Both ligands (IPTG and 40–base pair operator) were saturating and at concentrations at least 1,000-fold their dissociation constants.

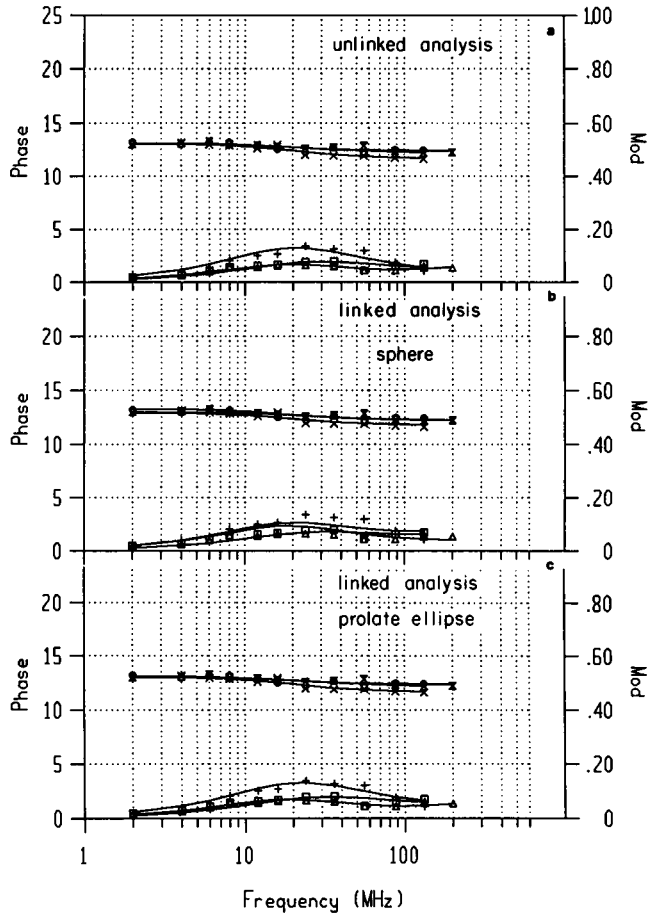

FIGURE 11 Differential phase and modulation between the parallel and perpendicular emission components for wild-type *lac* repressor (×, Mod; +, Phase), the W201Y mutant repressor (▽, Mod; □, Phase), and the W220Y mutant repressor (○, Mod; △, Phase). (*a*) Single curve analysis; (*b*) global analysis linking one long rotational rate with the fast rate unlinked; and (*c*) global analysis linking one fast rotational rate and two long rates corresponding to the long and short axes of a prolate ellipse. The preexponential weighting factors, β, were unlinked for both of the above global fits.

will show a longer average rotational correlation time than residues aligned along the short axis. To examine whether the observed changes in mean rotational correlation times originated from this type of "geometrical" effect, a global analysis was performed in which the data were analyzed directly in terms of a set of *internally consistent* overall protein motion(s) coupled to independent fast motions associated with each specific tryptophan residue. This analysis is essentially identical to the global analysis of multiple-dye studies on proteins previously described (40).

When a global analysis is performed in terms of only a single protein-tumbling rotational correlation time (and allowing each tryptophan to have its own fast librational

TABLE 4 Differential phase and modulation results from the wild-type and mutant *lac* repressor proteins: single curve analysis

Protein	ϕ_1	β_1	ϕ_2	β_2	χ^2
wild type	45	0.275	0.06	0.045	2.85
W201Y	57	0.257	0.09	0.063	3.80
W220Y	87	0.252	0.09	0.068	1.61

Excitation was at 295 nm. Emission was monitored using a WG320 cuton filter. The differential phase angle and modulation ratio between the parallel and perpendicular emission components as a function of frequency were analyzed as single curves in terms of two rotational rates, one for local tryptophan motions and the other due to the global tumbling of the protein particle.

motion) the recovered χ^2 value doubles with respect to the unlinked analysis, indicating that the spherical model is inappropriate. The data and fit are shown in Fig. 11 *b*. When a global analysis of the data is performed in terms of an internally consistent set of two slow rotational correlation times (associated with overall protein motion), the global χ^2 value decreases 50%, to a level identical with the unlinked analysis (Fig. 11 *c*). What these results show is that the molecular shape of the *lac* repressor cannot be represented as spherical, but rather requires that it be modeled as a prolate ellipsoid of revolution. (A more complicated model using a general ellipsoid could not be statistically justified.) The parameters recovered from this global analysis correspond to a fast rotational rate of 60 ps (associated with the local motions of the individual troptophans) and two tumbling rates of 21 and 82 ns for the entire protein motion (summarized in Table 5). If one assumes that these two rates correspond to rotations about the major and minor axes of a prolate ellipse, then these values can be used to calculate an apparent axial ratio for the *lac* tetramer. The axial ratio (a/b) calculated from the recovered correlation times is 3.1. Steitz and co-workers from neutron diffraction experiments report

TABLE 5 Differential phase and modulation results from the wild-type and mutant *lac* repressor proteins: global analysis results: $\chi^2 = 2.71$

Protein	ϕ_1	β_1	ϕ_2	β_2	ϕ_3	β_3	χ^2
Wild type	0.06	0.189	21	0.271	82	0.540	2.54
W201Y	0.06	0.258	21	—	82	0.752	4.03
W220Y	0.06	0.239	21	0.171	82	0.590	1.64

Excitation was at 295 nm. Emission was monitored using a WG320 cuton filter. The differential phase angle and modulation ratio between the parallel and perpendicular emission components as a function of frequency for all three proteins were analyzed simultaneously in terms of a consistent set of three rotational rates, one for local tryptophan motions and the other two due to the global tumbling of the protein particle around its long and short axes.

dimensions of 130–140 Å for the long axis and 55–65 and 45 Å for the short axes of the tetramer (41). The ratio of the long axis to the shorter of the other two is 3.0 and in strikingly good agreement with the value (3.1) calculated from the correlation times. Several other investigations using neutron diffraction (42–44) and low angle x-ray scattering (45, 46) have found elongated structures for the repressor with axial ratios between 2 and 3. It is interesting to note that the W201Y mutant data show essentially no contribution from the 21-ns rotational rate. If the two long rotational correlation times do, in fact, correspond to rotation about the longest and shortest axes of the tetramer, then the implication is that the excited-state dipole of tryptophan 220 is well aligned with the long axis of the tetramer.

Confidence intervals for the long rotational rates were essentially flat due to the strong correlation between the parameters of the fit, indicating that the errors in the recovered axial ratio are significant. However, there is little doubt that the anisotropic character of the *lac* repressor protein motion is being detected. Thus, whereas the conclusions from the results of the global analysis must be taken with caution, the data are *consistent* with the simplest interpretation; i.e., the fluorescence depolarization properties of the wild-type protein appear to result from a simple linear combination of the rotational behavior of the two-tryptophan residues oriented at different angles with respect to the principal diffusion axes of the protein. Although more complicated explanations of the observed effects are certainly possible, they are not explicitly required, and simple linear combination modeling (as performed for the total-intensity data) is consistent with the observed data. In addition, the recovered parameters from this simple model correlate very well with what is know about the structure of the *lac* repressor.

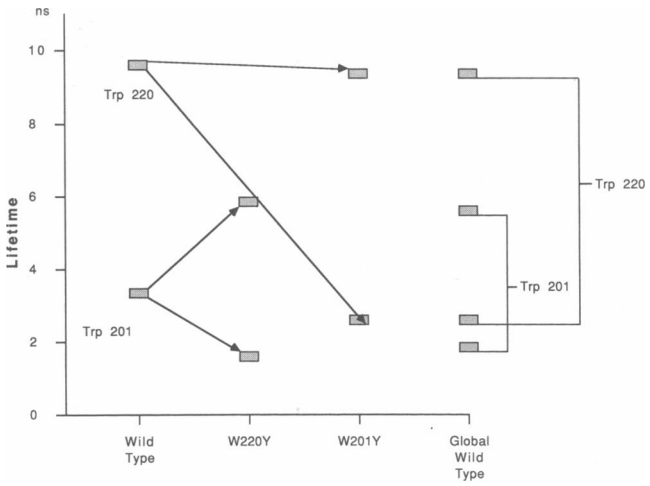

FIGURE 12 Schematic representation of the fluorescence decay from the wild-type *lac* repressor, the W201Y and W220Y mutants and the global analysis showing the decomposition of the wild-type decay into a combination of the four rates recovered from the mutant data.

DISCUSSION

Site-directed mutagenesis has provided the possibility of investigating whether the two components recovered from the analysis of the time-resolved fluorescence of a two-tryptophan protein actually correspond to the individual decays from the two tryptophans. We find that the situation is more complex; we diagramatically summarize it in Fig. 12. As in the case of most single-tryptophan proteins, the single-tryptophan mutants of the *lac* repressor display multiexponential decays. One of the recovered components is very long and thus well separated from all the others. It is therefore well resolved in the analysis of the wild-type data. Because the contribution of the long-lived component to the total wild-type signal is large, resolution of the shorter decay is more difficult. In fact, the shorter lifetime which is recovered from the wild type probably results from a combination of the other decay rates recovered for the individual tryptophan residues. If we analyze simultaneously all of the multiple emission wavelength data sets, mutants, and wild type together and force the wild-type fluorescence to be a linear combination of the fluorescence from the two mutants, the biexponential behavior of the wild-type protein can be decomposed into at least four exponentials. These results are contingent upon the hypothesis that the two tryptophans in the wild-type protein act independently of each other. The fluorescence lifetimes of the wild-type tryptophans have been found to be independent of excitation wavelength (295–305 nm) (data not shown), indicating that this hypothesis is reasonable.

We suspect that the case of the *lac* repressor is probably not an isolated one. The apparent double exponential decay of a number of two-tryptophan proteins, as well as the two to three classes of decays recovered for multiple-tryptophan proteins, will most likely prove to be the result of a superposition of the multiple decay rates of the individual tryptophan residues. It is important to note that the recovered parameters are independent of the data acquisition method (single photon counting or frequency domain) and of the method of data analysis (global nonlinear least-squares or maximum entropy). When studying such complex systems, it becomes apparent that one must obtain data along as many different experimental axes as possible. At the very minimum, multiple excitation/emission wavelengths need to be explored. Superimposed on this mimimal data set, additional axes such as multiple quenchers, multiple ligands, multiple temperatures (viscosities), etc., should be examined. Even

using such approaches, the rigorous resolution of the fluorescence decays of each tryptophan examining only wild-type multi-tryptophan-containing proteins will not necessarily be possible with the current fluorescence instrumentation and analysis techniques.

The rotational properties of the tryptophan residues in the *lac* repressor were found to be very similar. They both exhibited a small and rapid rotation in addition to depolarization due to the rotational diffusion of the macromolecule. Interestingly, we have recovered correlation times for this macromolecular tumbling which are quite consistent with the known ellipsoidal shape and dimensions of the *lac* tetramer, and the emission dipole of tryptophan 220 appears to be aligned with the long axis of the tetramer. The analysis would not have been so straightforward, however, had the degree of depolarization due to local rotations been greater or more complex for either of the two residues. In this latter case, accurate recovery of multiple rotational parameters would have undoubtedly proven less feasible.

The three major fluorescence signals, lifetime, energy, and anisotropy, of the two-tryptophan residues in the *lac* repressor have been characterized. In this case it appears that the energy of the emission corresponds reasonably well with the lifetime. The longer lifetime allows for a greater degree of solvent relaxation. Thus, the 9–10-ns component is red shifted with respect to the 5–6-ns component, which is itself red shifted with respect to the very fast decay rates. Protein structure, which determines the extent of exposure to the solvent, also plays an important role in determining the energy of emission. Thus, although the binding of inducer leads to a decrease in the lifetime of the 9-ns component to 7.4 ns (perhaps due to quenching by the sulfur of the sugar), the blue shift in the spectrum ($\sim$500 cm^{-1}) is much larger than warranted by the change in lifetime, indicating shielding of the tryptophan 220 upon ligand binding. The 30-fold decrease in inducer affinity in the W220Y mutant which has tyrosine in place of tryptophan 220 also indicates that this tryptophan may reside in the inducer binding site cleft and directly interact with the inducer (Gardner, J. A., and K. S. Matthews, manuscript in preparation). Comparison of the *lac* sequence with that of the galactose-binding protein (GBP) sugar-binding site demonstrates tryptophan in homologous positions in the two proteins (47) (Gardner, J. A., and K. S. Matthews, manuscript in preparation). In GBP, this tryptophan forms part of a sandwich for the sugar ligand (47). The environment of tryptophan 220 appears to be very different than that of tryptophan 201, in terms of lifetime, emission energy, and sensitivity of the emission energy to ligation. This apparent difference in energies and decay rates, however, is not correlated with any major differences in the rotational behavior. Both are rather rigidly held in the protein matrix, exhibiting very small and rapid depolarizations in addition to the depolarization due to the asymmetric global tumbling of the macromolecule. From these data, it does not appear that the rotational flexibility of the

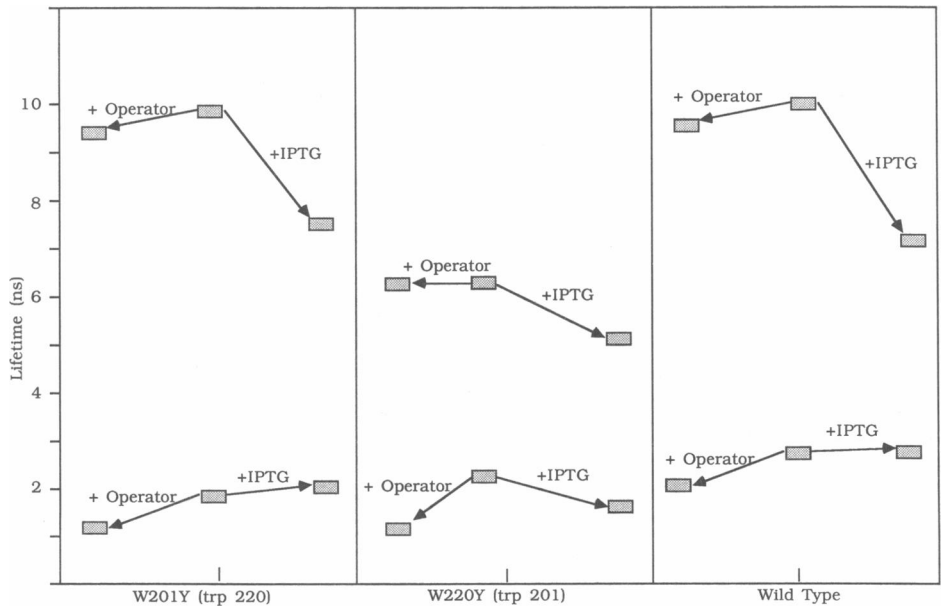

FIGURE 13 Schematic representation of the effect of ligation by saturating inducer, IPTG, and saturating 40-base pair operator on the decay parameters for the wild-type *lac* repressor and the two mutant proteins, W220Y and W201Y.

residues can be invoked as giving rise to their heterogeneous decay. It is also of interest that while the effects of ligation on the emission energy are very different for the two-tryptophan residues, they are very similar for the decay rates. This peculiar similarity in the effect of ligation on the decay rates is quite clear from examination of the diagram in Fig. 13. In all three cases, inducer binding had a larger effect on the long component(s) (an ~20% decrease), whereas operator binding resulted primarily in further quenching of the fast decay rates. Results such as these suggest that certain *global* properties of the protein's structure such as potential contours, helix dipole orientations, and charge distributions may be important in determining the observed decay of fluorescence. The state of ligation by the two antagonistic ligands could drive the equilibria between different conformations in which one or more of these general structural aspects is altered, giving rise to similar ligation effects on the decay kinetics for both tryptophan residues, which are only separated by amino acid–19 residues. Thus, the lifetime response of the two-tryptophan residues to ligation by the functionally important molecules of the *lac* repressor has been determined. To further clarify the relationships between fluoresence signals and function (which in this case is the state of ligation of the protein) the decay-associated spectra for the wild-type and the two single-tryptophan mutants is currently being undertaken as a function of ligation state. In addition, the effect of ligation on the rotational properties of the two-tryptophan residues is also being explored.

Clearly, the basis for multiple or distributed fluorescence decay rates in the asymmetric and heterogeneous environment of the protein matrix is not known. Differentiation of the decays using multiple data axes (i.e., temperature, pressure, ligands, and quenchers) will aid in sorting out the correlations between the various fluorescence parameters. We expect that site-directed mutagenesis will play an increasingly important role as the goal of these studies tends toward a more and more detailed understanding of the relations between structure, dynamics, function, and time-resolved fluorescence signals in biological molecules.

The authors would like to acknowledge the French Centre National pour la Recherche Scientifique (CNRS) for funding the travel expenses of Dr. Royer to L.U.R.E. In addition, we thank the technical staff at L.U.R.E. for running the synchrotron during the beam-time sessions. This work was also supported by National Institutes of Health grants to C. A. Royer (GM39969) and to K. S. Matthews (GM22441), as well as a Welch Foundation grant (C-576) to KSM and a Lucille B. Markey scholar award to JMB. The acquisition and analysis of the multifrequency data was carried out at the Laboratory for Fluorescence Dynamics at the University of Illinois at Urbana-Champaign. The Laboratory for Fluorescence Dynamics is jointly supported by the Division of Research Resources of the National Institutes of Health and the University of Illinois.

Received for publication 13 November 1989 and in final form 16 April 1990.

REFERENCES

1. Beechem, J. M., and L. Brand. 1985. Time resolved fluorescence of proteins. *Annu. Rev. Biochem.* 54:43–71.
2. Neyroz, P., J. M. Beechem, L. Brand, and S. Roseman. 1984. Nanosecond time resolved fluorescence decay studies of the temperature dependent association of enzyme I of bacterial phosphotransferase system. *Photochem. Photobiol.* 39:41S.
3. Knutson, J. R., D. G. Walbridge, and L. Brand. 1982. Decay associated fluorescence spectrum and the heterogeneous emission of alcohol dehydrogenase. *Biochemistry.* 21:4671–4679.
4. Ross, J. B. A., C. J. Schmidt, and L. Brand. 1981. Time-resolved fluorescence of the two tryptophans in horse liver alcohol dehydrogenase. *Biochemistry.* 20:4369–4377.
5. Brochon, J. C., P. Wahl, M. Charlier, J. C. Maurizot, and C. Hélène. 1977. Time resolved fluorescence of the tryptophyl residues of the *E. coli lac* repressor. *Biochim. Biophys. Res. Commun.* 79:1261–1271.
6. Privat, J. P., P. Wahl, and J. C. Auchet. 1980. Time-resolved spectroscopy of tryptophyl fluorescence of yeast 3-phospho glycerate kinase. *Biophys. Chem.* 11:239–248.
7. Gafni, A., and M. M. Werber. 1979. Ferridoxin from *Halobacterium* of the dead sea: structural properties revealed by fluorescence techniques. *Arch. Biochem. Biophys.* 196:363–370.
8. Hochstrasser, R. M., and D. K. Negus. 1984. Picosecond decay of tryptophans in myoglobin. *Proc. Natl. Acad. Sci. USA.* 81:4399–4403.
9. Royer, C. A., P. Tauc, G. Hervé, and J. C. Brochon. 1987. Ligand binding and protein dynamics: a fluorescence depolarization study of aspartate transcarbamylase from *Escherichia coli. Biochemistry.* 26:6472–6478.
10. Mérola, F., R. Rigler, A. Holmgren, and J. C. Brochon. 1989. Picoscond tryptophan fluorescence of thioredoxin: evidence for discrete species in slow exchange. *Biochemistry.* 28:3383–3398.
11. Munro, I., I. Pecht, and L. Stryer. 1979. Subnanosecond motions of tryptophan residues in proteins. *Proc. Natl. Acad. Sci. USA.* 76:56–60.
12. Szabo, A. G., T. M. Stepanik, D. M. Wayner, and N. M. Young. 1983. Conformational heterogeneity of the copper binding site in azurin: a time-resolved fluorescence study. *Biophys. J.* 411:233–244.
13. Cockle, S. A., and A. G. Szabo. 1981. Time resolved fluorescence spectroscopy of tryptophan in monomeric glucagon. *Photochem. Photobiol.* 34:23–27.
14. Grinvald, A., and I. Z. Steinberg. 1976. The fluorescence decay of tryptophan residues in native and denatured proteins. *Biochim. Biophys. Acta.* 427:663–678.
15. De Lauder, W. V., and P. Wahl. 1971. Fluorescence studies on human serum albumin. *Biochim. Biophys. Res. Commun.* 42:398–404.
16. Jonas, A., J. Privat, P. Wahl, and J. C. Osborne, Jr. 1982. Nanosecond rotational motions of apo-lipoprotein CI in solution and in complexes with dimyristoylphosphatidyl choline. *Biochemistry.* 21:6205–6211.

17. Lee, J., D. J. O'Kane, and A. J. W. G. Visser. 1985. Spectral properties and function of two lumazine proteins from photobacterium. *Biochemistry.* 24:1476–1483.

18. Vincent, M., J. C. Brochon, F. Mérola, W. Jordi, and J. Gallay. 1988. Nanosecond dynamics of horse heart apocytochrome *c* in aqueous solution as studied by time-resolved fluorescence of the single tryptophan residue (Trp-59). *Biochemistry.* 27:8752–8761.

19. Royer, C. A., A. E. Chakerian, and K. S. Matthews. 1990. Macromolecular binding equilibria in the *lac* repressor system: studies using high pressure fluorescence spectroscopy. *Biochemistry.* In press.

20. Royer, C. A. 1985. The use of high pressure fluorescence spectroscopy to investigate subunit interactions in oligomeric proteins. Ph.D. thesis. University of Illinois. Urbana-Champaign.

21. Sommer, H., P. Lu, and J. H. Miller. 1976. *Lac* repressor: fluorescence of the two tryptophans. *J. Biol. Chem.* 251:3774–3779.

22. Kunkel, T. A. 1985. Rapid and efficient site-specific mutagenesis without phenotypic selection. *Proc. Natl. Acad. Sci. USA.* 82:488–492.

23. Dente, L., G. Cesareni, and R. Coltrese. 1983. pEMBL: a new family of single-stranded plasmids. *Nucleic Acids Res.* 11:1645–1655.

24. Sanger, F., A. R. Coulson, B. G. Barell, A. J. H. Smith, and B. A. Roe. 1980. Cloning in single-stranded bacteriophage as an aid to rapid DNA sequencing. *J. Mol. Biol.* 143:161–178.

25. O'Gorman, R. B., M. Dunaway, and K. S. Matthews. 1980. DNA binding characteristics of lactose repressor and the trypsin-resistant core repressor. *J. Mol. Biol.* 255:10100–10106.

26. Ware, W. R. 1971. Creation and Detection of the Excited State. Vol. 1. Marcel Dekker, Inc., New York. 213–302.

27. Yguerabide, J. 1972. Nanosecond fluorescence spectroscopy of macromolecules. *Methods Enzymol.* 29:498–578.

28. Wahl, P. 1975. Nanosecond pulse fluorometry. *In* New Techniques in Biophysics and Cell Biology. Vol. 2. M. Pain, and J. Smith, editors. John Wiley & Sons, Inc., 233–285.

29. Jameson, D. M., and B. Alpert. 1979. Synchrotron radiation applied to biophysical and biochemical research *In* Synchrotron Radiation Applied to Biophysical and Biochemical Research. A. Castellani and J. F. Garcia, editors. Plenum Publishing Corp., New York. 183–201.

30. Brochon, J. C. 1980. Protein Dynamics and Energy Transduction. I. Shin'lchi, editor. Taniguchi Foundation, Tokyo. 163–189.

31. Mérola, F., and J. C. Brochon. 1986. Polarized pulse fluorometry study on the conformational properties of wheat germ hexokinase I. *Eur. Biophys. J.* 13:291–299.

32. Alcala, J. R., E. Gratton, and D. M. Jameson. 1985. A multifrequency phase fluorometer using the harmonic content of a mode-locked laser. *Anal. Instrum.* 14:225–231.

33. Knutson, J. R., J. M. Beechem, and L. Brand. 1983. Simultaneous analysis of multiple fluorescence decay curves: a global approach. *Chem. Phys. Lett.* 102:501–507.

34. Beechem, J. M., J. R. Knutson, J. B. A. Ross, B. W. Turner, and L. Brand. 1983. Global resolution of heterogeneous decay by phase/modulation fluorometry: mixtures and proteins. *Biochemistry.* 22:6054–6058.

35. Beechem, J. M., and E. Gratton. 1988. Fluorescence spectroscopy data analysis environment: a second generation global analysis program. *Proc. SPIE.* 909:70–81.

36. Beechem, J. M., E. Gratton, M. A. Ameloot, J. R. Knutson, and L. Brand. 1989. The global analysis of fluorescence intensity and anisotropy decay data: second generation theory and programs. *In* Fluorescence Spectroscopy. Vol. I. Principles and Techniques. J. R. Lakowicz, editor. Plenum Publishing Corp., New York. In press.

37. Livesey, A. K., and J. C. Brochon. 1987. Analyzing the distribution of decay constants in pulse fluorometry using the maximum entropy method. *Biophys. J.* 52:693–706.

38. Skilling, J., and R. K. Bryan. 1984. Maximum entropy image reconstruction: general algorithm. *Mon. Not. R. Astr. Soc.* 211:111–124.

39. Livesey, A. K., and J. Skilling. 1985. Maximum entropy theory. *Acta Crystallogr. Sect. B. Struct. Crystallogr. Cryst. Chem.* A41:113–122.

40. Beechem, J. M., J. R. Knutson, and L. Brand. 1987. Global analysis of multiple dye fluorescence anisotropy experiments on protein. *Trans. Biochem. Soc.* 14:832–835.

41. Steitz, T. A., T. J. Richmond, D. Wise, and D. Engelman. 1974. The *lac* repressor protein: molecular shape, subunit structure, and proposed model for operator interaction based on structural studies of microcrystals. *Proc. Natl. Acad. Sci. USA.* 71:593–597.

42. Charlier, M., J. Zaccai, and J. C. Maurizot. 1979. Neutron scattering study of *lac* repressor and of its tryptic core. *In* Fifth EMBO Annual Symposium: Nucleic Acid-Protein Interactions. IRL Press Ltd., Oxford, UK. 337.

43. Charlier, M., J. C. Maurizot, and J. Zaccai. 1980. Neutron scattering studies of *lac* repressor. *Nature* (*Lond.*). 286:423–424.

44. Charlier, M., J. C. Maurizot, and J. Zaccai. 1981. Neutron-scattering studies of *lac* repressor: a low-resolution model. *J. Mol. Biol.* 153:177–182.

45. Pilz, I., K. Goral, O. Kratky, N. G. Wade-Jaredetzky, and O. Jaredetzky. 1980. Small-angle x-ray studies of the quaternary structure of the *lac* repressor from *Escherichia coli. Biochemistry.* 19:4087–4090.

46. McKay, D. B., C. A. Pickover, and T. A. Steitz. 1982. *Escherichia coli lac* repressor is elongated with its operator DNA binding domains located at both ends. *J. Mol. Biol.* 156:175–183.

47. Vyas, N. K., M. N. Vyas, and F. A. Quiocho. 1988. Sugar signal transducer binding sites of the *Escherichia coli* galactose chemoreceptor protein. *Science* (*Wash. DC*). 242:290–295.